ISSN 2278-2540 | DOI: 10.51583/IJLTEMAS | Volume XV, Issue II, February 2026

Synthesis and Characterization of Methanolic Root Extract of Imperata Cylindrica and Its Nanoencapsulation with Chitosan

P. O. Okwuego[1]*, V. O. Offiah[1], C. M. Okey-Nzekwe[1]

Department of Pure and Industrial Chemistry, Chukwuemeka Odumegwu Ojukwu University, Anambra State, Nigeria

***Corresponding Author**

DOI: https://doi.org/10.51583/IJLTEMAS.2026.15020000108

Received: 25 February 2026; Accepted: 02 March 2026; Published: 20 March 2026

ABSTRACT

The development of efficient nano-based drug delivery systems remains a critical strategy for improving the stability, bioavailability, and therapeutic performance of plant-derived bioactive compounds. In this study, methanolic root extract of *Imperata cylindrica* was synthesized, characterized, and nanoencapsulated using chitosan as a biodegradable and biocompatible polymeric carrier, with the objective of enhancing its suitability for wound-healing and hemostatic drug delivery applications. Qualitative and quantitative phytochemical analyses revealed the presence of alkaloids (5.4%), tannins (5.7%), flavonoids (10.3%), saponins (2.25%), and terpenoids (43.3%), which are compounds commonly associated with anti-inflammatory, antimicrobial, and tissue-repair activities. Nanoencapsulation was achieved via chitosan-assisted precipitation, and the resulting nanoparticles were characterized using Fourier transform infrared spectroscopy (FTIR), ultraviolet–visible (UV–Vis) spectroscopy, transmission electron microscopy (TEM), and X-ray diffraction (XRD). FTIR spectra confirmed the successful incorporation of the extract within the chitosan matrix through the presence of characteristic O–H, N–H, and C=O functional groups without structural degradation. TEM analysis revealed predominantly spherical, mesoporous nanoparticles with particle sizes ranging from 2 to 50 nm and average diameters between 12.66 and 17.98 nm. UV–Vis spectroscopy demonstrated a hypsochromic shift in absorption maxima from 550 nm for the free extract to 375 nm for the nanoencapsulated formulation, indicating improved molecular dispersion and an encapsulation efficiency of 31.81%. XRD analysis revealed crystalline phases containing mineral oxides relevant to biological and pharmaceutical applications. Overall, the chitosan-based nanoencapsulation of *Imperata cylindrica* root extract demonstrates significant potential as a natural product-derived drug delivery system for topical wound-healing and hemostatic applications, aligning with current advances in polymeric nanoparticle-mediated drug delivery.

Keywords: *Imperata cylindrica*; chitosan nanoparticles; drug delivery system; nanoencapsulation; wound healing; hemostatic agents

INTRODUCTION

Efficient drug delivery remains a major challenge in pharmaceutical science, particularly for bioactive compounds derived from medicinal plants that often suffer from poor stability, low aqueous solubility, and limited bioavailability. Nano-enabled drug delivery systems have emerged as effective tools for overcoming these limitations by enhancing drug protection, controlled release, and targeted delivery to diseased tissues. Polymeric nanoparticles, especially those derived from natural polymers, are of increasing interest due to their favorable safety profiles and tunable physicochemical properties Agnihotri *et al* (2004).

Imperata cylindrica is a perennial rhizomatous grass widely distributed across tropical and subtropical regions and extensively used in traditional medicine for wound healing, hemostatic activity, anti-inflammatory effects, and treatment of liver disorders. Phytochemical studies have shown that the plant contains flavonoids, terpenoids, alkaloids, tannins, and glycosides, which contribute to its pharmacological activities. However, the

ISSN 2278-2540 | DOI: 10.51583/IJLTEMAS | Volume XV, Issue II, February 2026

direct application of crude plant extracts is often limited by instability, rapid degradation, and uncontrolled release at the site of action Alonso *et al* (2003); Cui et *al* (2012); Chen *et al.* (2016); Chen *et al.* (2015).

Chitosan, a cationic polysaccharide obtained through the deacetylation of chitin, has gained prominence in drug delivery science due to its biocompatibility, biodegradability, low toxicity, mucoadhesive behavior, and inherent antimicrobial properties. Chitosan-based nanoparticles are particularly attractive for topical and transdermal drug delivery owing to their ability to enhance drug retention, promote tissue interaction, and facilitate sustained release Ahmed *et al* (2016).

The present study focuses on the development of a chitosan-based nanoencapsulated formulation of methanolic root extract of *Imperata cylindrica*. The work emphasizes nanoparticle synthesis, physicochemical characterization, phytochemical profiling, and structural evaluation in the context of drug delivery science. By integrating traditional medicinal knowledge with modern nanotechnology, this study aims to provide a scientifically validated nano-drug delivery platform suitable for wound-healing and hemostatic applications Ali *et al* (2018).

MATERIALS AND METHODS

Sample Collection and Preparation

Fresh roots of *Imperata cylindrica* were collected from Umuenechi Village, Nibo, Anambra State, Nigeria. The plant was authenticated at the National Root Crops Research Institute Herbarium, Umudike, Abia State. The roots were washed, air-dried at room temperature for seven days, pulverized, and stored in airtight containers for subsequent analysis.

Extraction of Root Sample

One hundred and fifty grams (150 g) of the powdered root sample was macerated in 250 mL of methanol for 24 h. The extract was filtered using muslin cloth and concentrated to near dryness using a water bath at 70 °C. The concentrated extract was cooled and stored under refrigeration.

Synthesis of Chitosan

Chitosan was prepared via alkaline deacetylation of chitin obtained from carbonated periwinkle shells. The shells were activated using 0.5 M phosphoric acid, washed to neutral pH, oven-dried at 70 °C, and stored for nanoparticle synthesis.

Preparation of Nanoencapsulated Extract

One gram (1 g) of the methanol extract was dissolved in 150 mL of deionized water and added dropwise to 250 mL of 0.5 M ferric nitrate under continuous stirring. Chitosan (10 g per 100 mL of mixture) was subsequently introduced, and the mixture was stirred until gelation occurred. The product was concentrated at 65 °C, oven-dried, and stored for characterization.

RESULTS AND DISCUSSION

Organoleptic and Formulation Stability Assessment

The organoleptic evaluation of *Imperata cylindrica* root, chitosan, and the encapsulated particles revealed distinct differences in colour, texture, taste, and odour, reflecting their intrinsic properties and the effects of nanoencapsulation (Table 1). The root of *I. cylindrica* exhibited a milky colour, fine texture, mildly sweet taste, and mild odour, consistent with its natural plant composition and high phytochemical content. Chitosan appeared ash-coloured, powdery, with a shelly taste and soapy odour, typical of its polysaccharide structure. The encapsulated particles displayed a brown colour, prickly texture, sour taste, and pungent but non-choking odour,

ISSN 2278-2540 | DOI: 10.51583/IJLTEMAS | Volume XV, Issue II, February 2026

indicating successful integration of the extract into the polymer matrix. Importantly, the organoleptic properties of the nanoencapsulated formulation showed no observable deterioration in colour, odour, texture, or consistency throughout the analysis period. This stability highlights the protective role of the chitosan matrix, which preserves the bioactive constituents, maintains uniform sensory attributes, and enhances formulation robustness a critical factor for topical or oral drug delivery systems where consistency influences physicochemical stability and patient compliance Nkachukwu. *et al* (2025); Mmuo *et al* (2024); Okwuego, *et al* (2025).

Table 1. Organoleptic Properties of *Imperata cylindrica,* Chitosan, and Encapsulated Particles

Parameter	*Imperata cylindrica* Root	Chitosan	Encapsulated Particles
Colour	Milk	Ash	Brown
Texture	Fine	Powdery	Prickly
Taste	Sugary	Shelly	Sour
Odour	Mild	Soapy	Pungent but not choking

Morphological Characteristics and Particle Size Distribution

Transmission electron microscopy (TEM) analysis demonstrated that the nanoencapsulated *Imperata ylindrica*extract consisted predominantly of spherical nanoparticles with mesoporous structures and particle sizes ranging from 2 to 50 nm. The average particle sizes (12.66–17.98 nm) fall within the optimal range reported for polymeric nanoparticles intended for drug delivery applications Okwuego *et al* (2021); Ochie *et al* (2025); Okwuego (2025). Nanoparticles within this size regime are known to exhibit enhanced surface area, improved tissue interaction, and prolonged retention at the site of application, particularly in topical and wound-healing formulations.

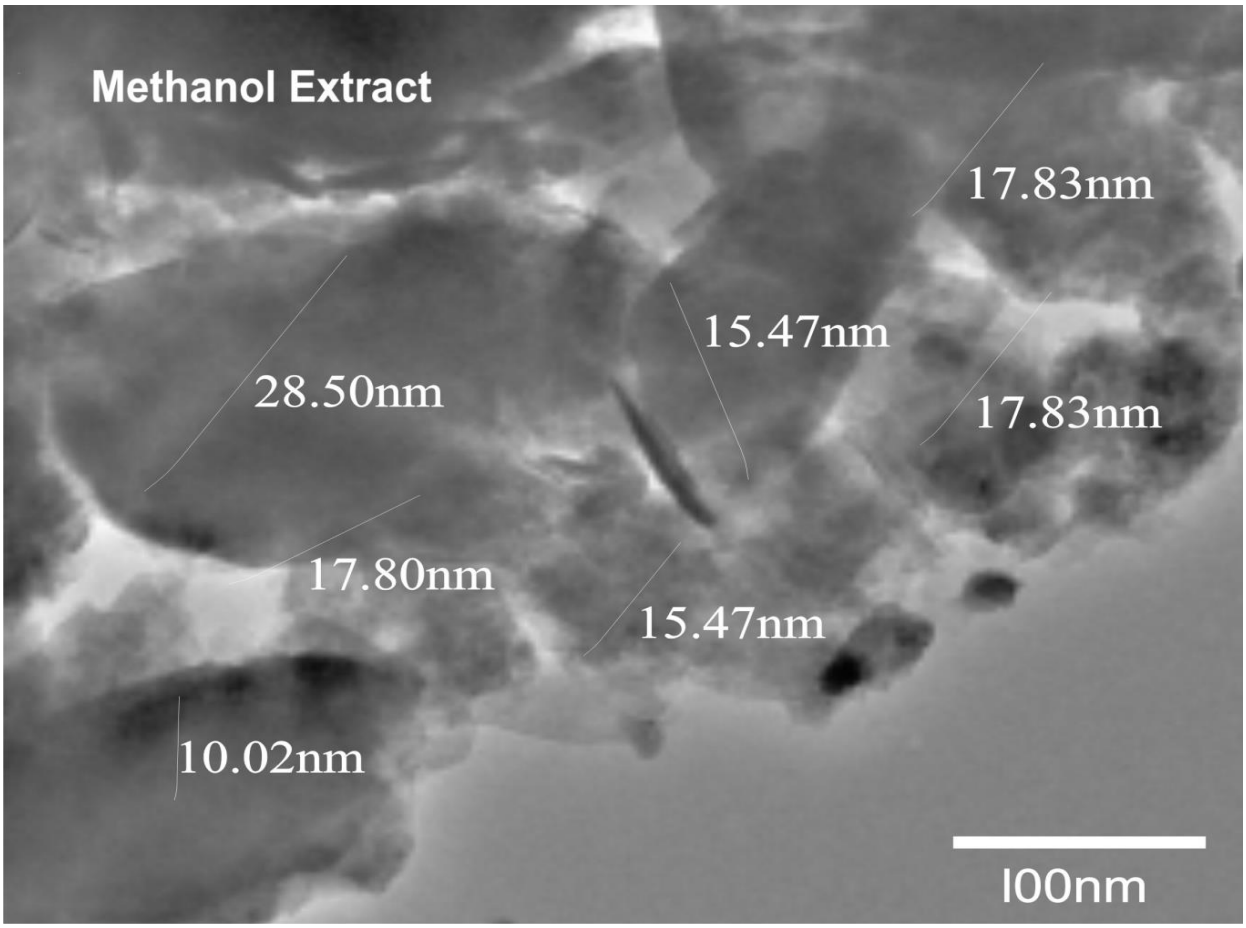

Figure 1 Transmission of Electron Microscope of Methanol Extract

ISSN 2278-2540 | DOI: 10.51583/IJLTEMAS | Volume XV, Issue II, February 2026

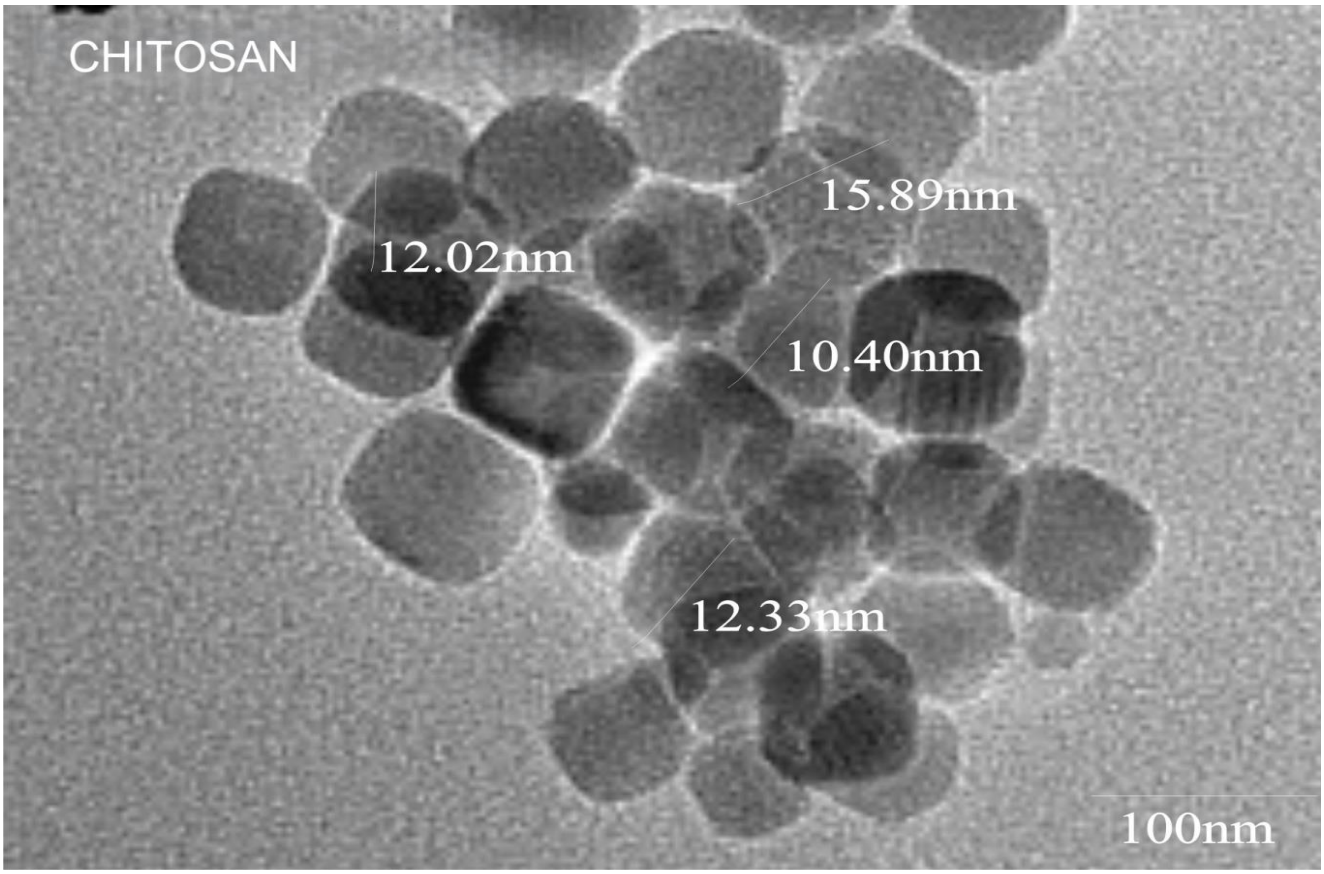

Figure 2 Transmission Electron Microscope of Chitosan

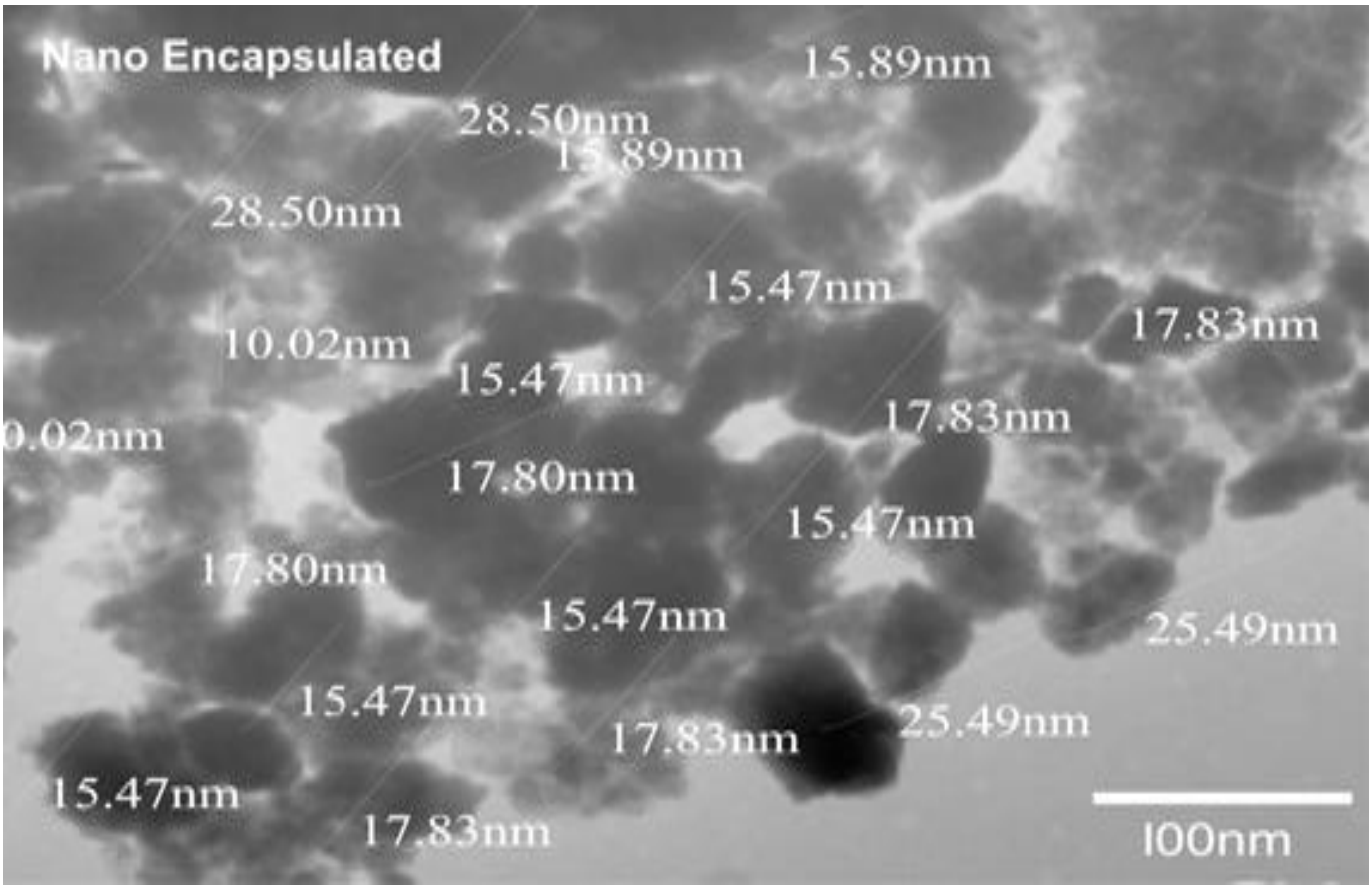

Figure 3 Transmission Electron Microscope of Encapsulated particle

ISSN 2278-2540 | DOI: 10.51583/IJLTEMAS | Volume XV, Issue II, February 2026

Compared with larger micro-scale carriers, the observed nanoscale dimensions are advantageous for facilitating intimate contact with damaged tissue surfaces and for promoting uniform drug distribution.

Mild particle agglomeration observed in some regions is consistent with previous reports on chitosan-based nanoparticles and may be attributed to intermolecular hydrogen bonding; however, the extent of agglomeration observed is unlikely to compromise delivery efficiency.

FTIR Analysis and Encapsulation Confirmation

FTIR analysis of *Imperata cylindrica* methanol extract (Table 2), chitosan (Table 3), and the encapsulated particles (Table 4) revealed the presence and preservation of key functional groups throughout the formulation process. The extract exhibited characteristic **O–H and N–H stretches** (3218–3498 cm^{-1}), **C=O stretches** (1618–1863 cm^{-1}), **C–O stretches** (1135–1295 cm^{-1}), **C–H stretches** (3013 cm^{-1}), and minor **C≡N peaks** (2016–2798 cm^{-1}), consistent with alkaloids, flavonoids, tannins, and terpenoids. Chitosan displayed broad O–H and amide N–H stretches (3245–3426 cm^{-1}), C=O stretches (1613–1884 cm^{-1}), and C–O stretches (1277–1415 cm^{-1}), reflecting its polysaccharide structure capable of hydrogen bonding.

The encapsulated particles retained all major extract and polymer peaks, with slight shifts in O–H and N–H bands (3141–3548 cm^{-1}) indicative of hydrogen bonding between the extract and chitosan matrix. Preservation of C=O, C–O, and C–H vibrations confirms that the bioactive compounds remain chemically intact after encapsulation Okwuego (2023); Ochie *et al* (2025); Okwuego *et al* (2021); Okwuego *et al* (2025)The FTIR results demonstrate successful incorporation of the extract into chitosan particles without chemical degradation, supporting the formulation's potential as a stable, natural product-based drug delivery system Ochie *et al* (2025); Okorie *et al* (2025)

Table 2. FTIR Spectral Data for *Imperata cylindrica* Methanol Extract

Frequency (cm^{-1})	**Functional Group / Assignment**
804.51	C–O, C–H deformation bonds for alkyl and methyl groups
892.10	C–O, C–H deformation bonds for alkyl and methyl groups
1039.88	C–H, C–O deformation bonds for alkyl groups
1134.69	**C–O deformation bonds for ketones and acids**
1294.83	**C–O stretch for ketones and alcohols**
1618.09	**C=O stretch for ketones, acids, and amides**
1863.65	C=O stretch for ketones, acids, and amides
2016.14	C≡N stretch for nitriles
2114.99	C≡N stretch for nitriles
2457.32	C≡N stretch for nitriles
2639.50	C≡N stretch for nitriles
2798.64	C≡N stretch for nitriles
3012.92	C–H stretch for alkenes
3218.10	**O–H stretch for alcohols, amides, and acids**
3313.14	**N–H and O–H stretch for amines, alcohols, and phenols**
3498.28	**O–H stretch for alcohols, acids, and amides**

ISSN 2278-2540 | DOI: 10.51583/IJLTEMAS | Volume XV, Issue II, February 2026

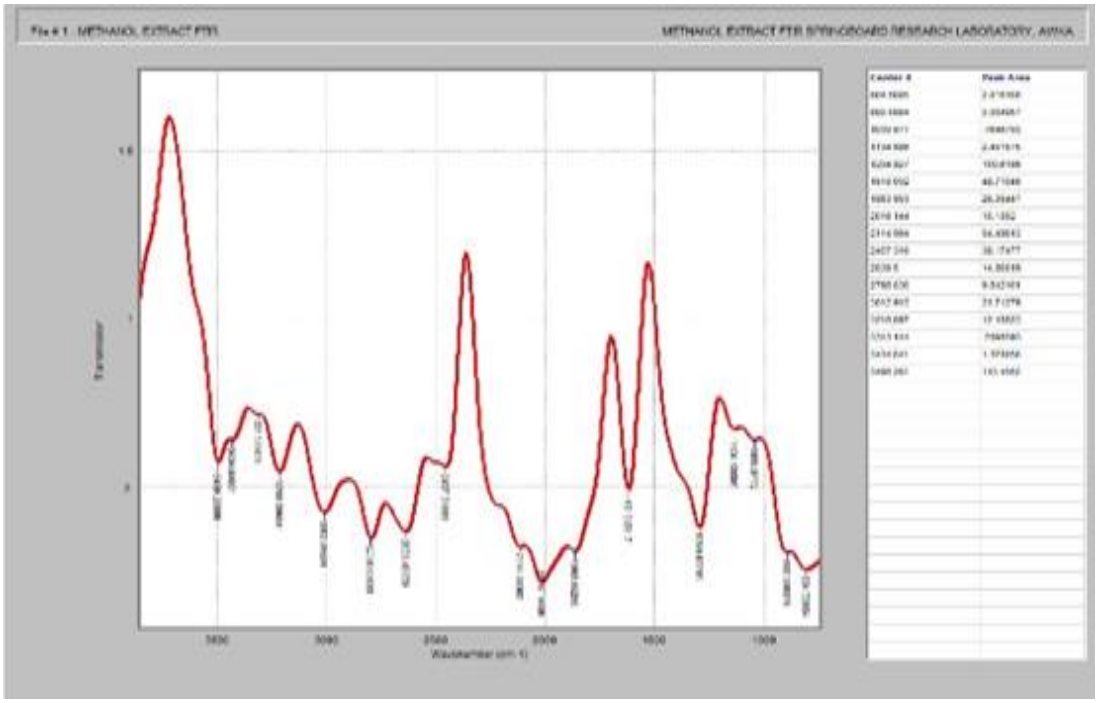

Figure 4 FTIR Spectra of Methanol extract

Table 3. FTIR Spectral Data for Chitosan Extract

Frequency (cm^{-1})	**Functional Group / Assignment**
745.89	C–O, C–H deformation bonds for alkyl and methyl groups
872.51	C–O, C–H deformation bonds for alkyl and methyl groups
1002.23	C–H, C–O deformation bonds for alkyl groups and ketones
1277.11	**C–O stretch for ketones and alcohols**
1414.91	**C–O stretch for ketones and alcohols**
1613.17	**C=O stretch for ketones, acids, and amides**
1752.35	C=O stretch for ketones, acids, and amides
1883.70	C=O stretch for ketones, acids, and amides
2106.59	C≡N stretch for nitriles
2210.17	C≡N stretch for nitriles
2450.63	C≡N stretch for nitriles
2538.17	O–H stretch for acids
2660.28	O–H stretch for acids
2761.99	C–H stretch for alkanes
2975.52	C–H stretch for alkenes
3244.61	**O–H stretch for alcohols, acids, and amides**
3426.32	**O–H stretch for alcohols, acids, and amides**
3800.54	O–H (unbound)

ISSN 2278-2540 | DOI: 10.51583/IJLTEMAS | Volume XV, Issue II, February 2026

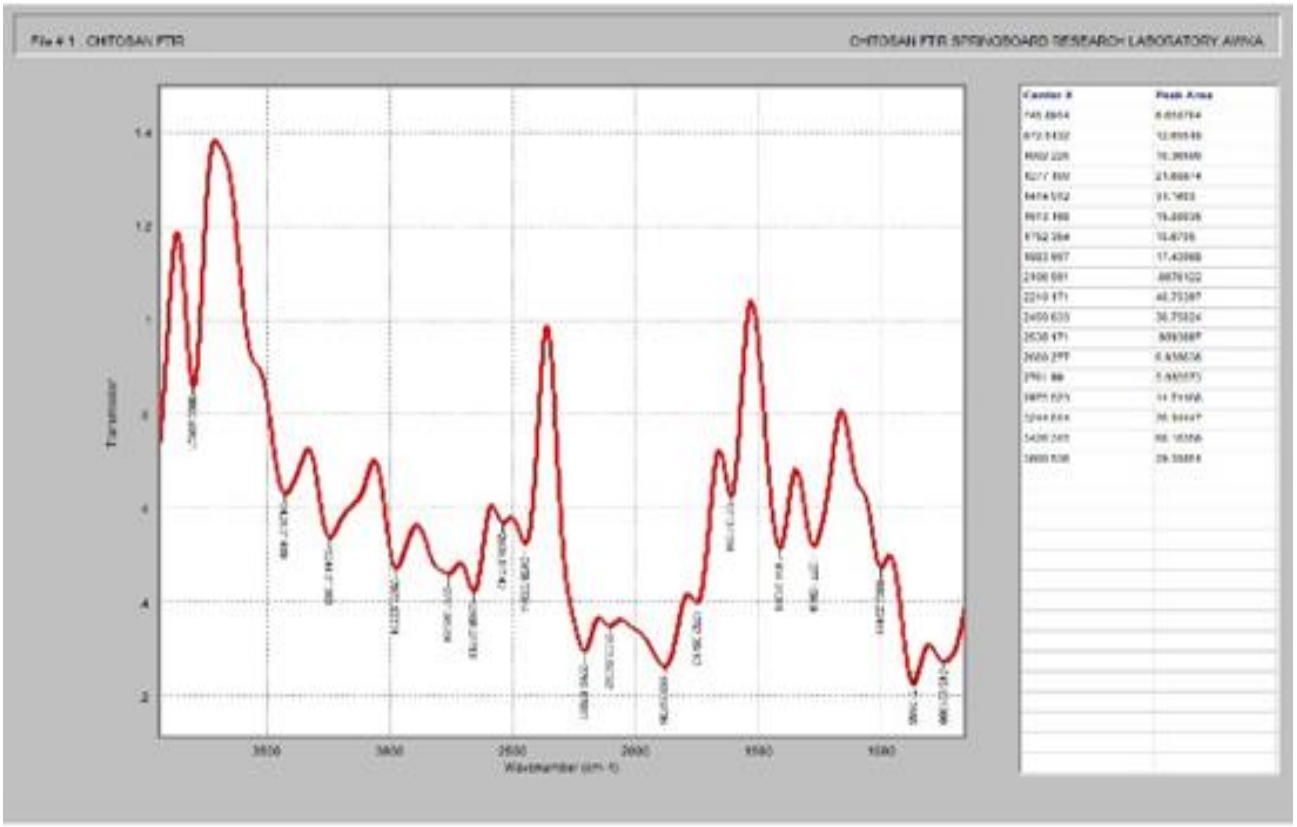

Figure .5 FTIR Spectra of Chitosan

Table 4. FTIR Spectral Data of Encapsulated Particles

Frequency (cm^{-1})	Functional Group / Assignment
839.80	C–O, C–H deformation bonds for alkyl and methyl groups
1016.40	C–O, C–H deformation bonds for alkyl groups and ketones
1400.32	**C–O stretch for ketones and acids**
1633.70	**C=O stretch for ketones and amide groups**
1871.38	C=O stretch for ketones, acids, and amides
2117.08	C≡N stretch for nitriles
2275.43	C≡N stretch for nitriles
2450.16	C≡N stretch for nitriles
2526.01	C≡N stretch for nitriles
2631.72	C–H stretch for alkenes and aromatic groups
2830.92	C–H stretch for alkenes and aromatic groups
2954.72	C–H stretch for alkanes, alkenes, acids, and aromatics
3045.69	C–H stretch for alkenes
3140.57	**N–H and O–H stretch for amines, alcohols, and phenols**
3261.19	**O–H stretch for alcohols, amides, and acids**
3548.20	**O–H stretch for alcohols, acids, and amides**
3698.69	O–H unbound for alcohols
3828.11	O–H unbound

ISSN 2278-2540 | DOI: 10.51583/IJLTEMAS | Volume XV, Issue II, February 2026

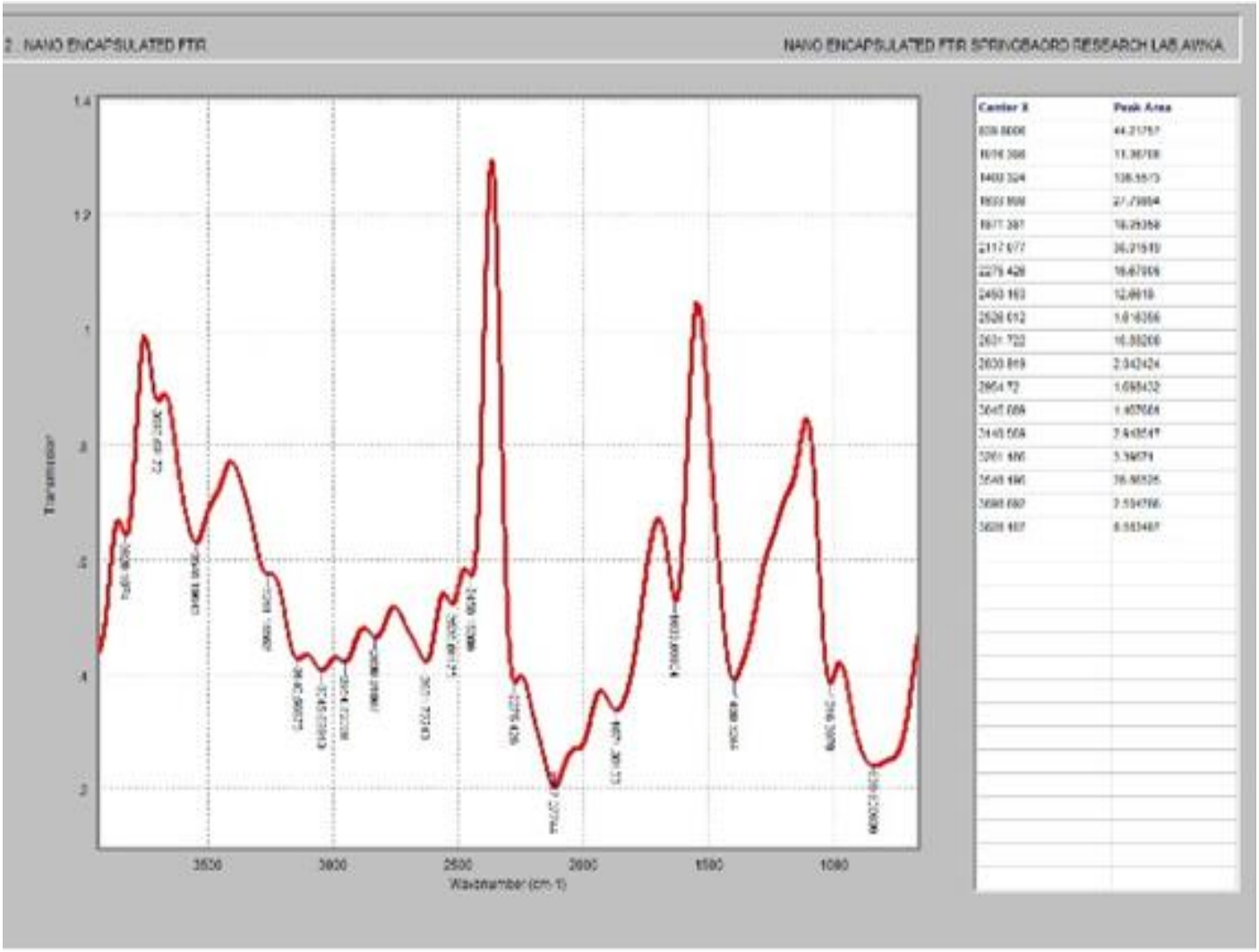

Figure .6 FTIR SPECTRA of Encapsulated particle.

Importantly, no disappearance or excessive shifting of major peaks was observed following encapsulation, indicating that the structural integrity of the bioactive phytochemicals was preserved. This observation is particularly significant for drug delivery systems, as chemical alteration of active compounds during formulation can compromise therapeutic efficacy.

UV–Visible Spectroscopy and Encapsulation Efficiency

UV-Vis analysis of chitosan, the methanol extract of *Imperata cylindrica*, and the encapsulated extract (Table 5) revealed distinct absorption patterns and structural interactions within the polymer matrix. Chitosan exhibited low, nearly constant absorbance across 350–850 nm, consistent with its polysaccharide structure and absence of strong chromophores. The methanol extract showed a pronounced peak at 500–600 nm, attributed to $\pi \rightarrow \pi^*$ transitions in conjugated systems such as flavonoids, terpenoids, and polyphenols. Upon nanoencapsulation, the extract displayed substantially reduced absorbance across all wavelengths, with a hypsochromic shift of the absorption maximum from 550 nm for the free extract to 375 nm in the encapsulated formulation. This blue shift indicates reduced molecular aggregation and improved dispersion of the bioactive compounds within the chitosan matrix Nkachukwu. *et al* (2025); Mmuo *et al* (2024); Okwuego, *et al* (2025). The calculated encapsulation efficiency of 31.81% demonstrates effective incorporation of the extract, comparable to other chitosan-based plant bioactive formulations. The diminished optical activity and similarity in absorption behavior between chitosan and the encapsulated particles confirm successful entrapment and compatibility of the polymer drug system. From a drug delivery perspective, these spectral features suggest enhanced stability, controlled presentation of active constituents, and potential for improved bioavailability and sustained release at the wound site.

ISSN 2278-2540 | DOI: 10.51583/IJLTEMAS | Volume XV, Issue II, February 2026

Table 5. Absorbance per Unit Wavelength of Chitosan, Methanol Extract, and Encapsulated Extract of *Imperata cylindrica*

Wavelength (nm)	Chitosan	Methanol Extract of *I. cylindrical*	Encapsulated Extract of *I. cylindrical*
350	0.344	1.758	0.107
400	0.344	1.762	0.107
450	0.274	2.225	0.039
500	0.250	6.000	0.017
550	0.202	6.000	-0.002
600	0.182	6.000	-0.008
650	0.149	0.850	-0.011
700	0.133	0.535	-0.012
750	0.122	0.345	-0.014
800	0.110	0.241	-0.014
850	0.100	0.180	-0.015

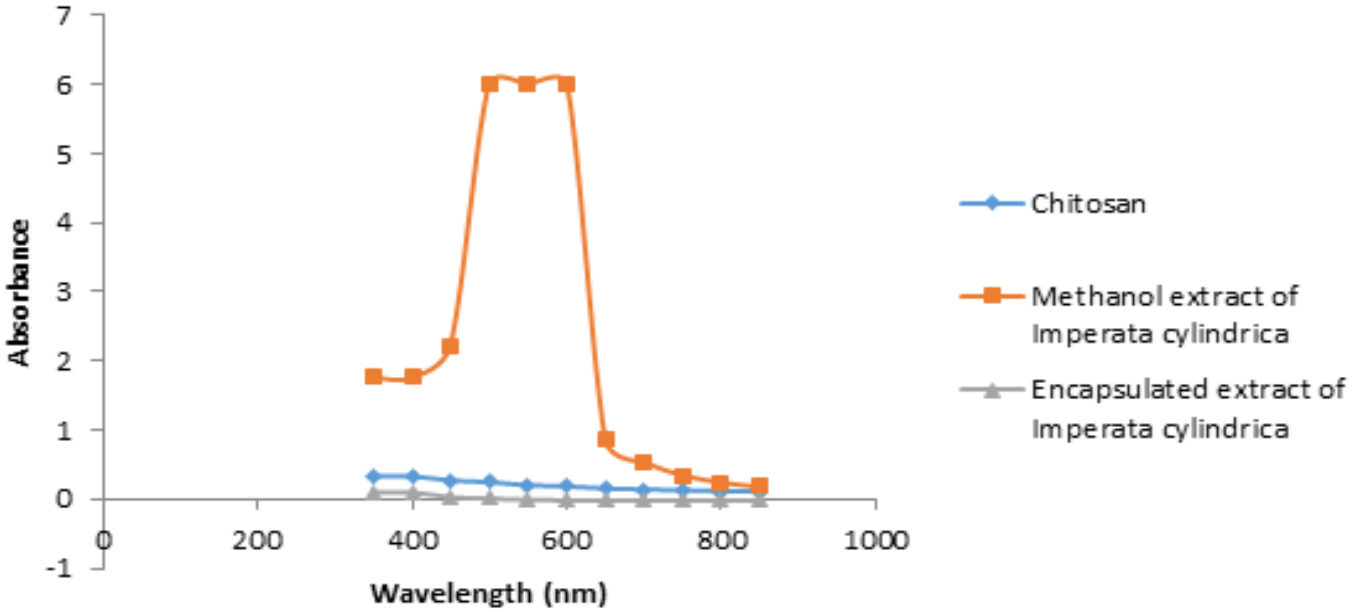

Figure 7Absorption maxima of the various sample

3.5 Crystallinity and Mineral Composition Analysis by XRD

X-ray diffraction (XRD) analysis of the encapsulated nanoparticles (Tables 6 and 7)revealed a multi-phase crystalline composition consisting of Barium Terbium Niobium Oxide (Ba_2TbNbO_6), Romarchite (SnO), Ziroite (ZrO_2), Freibergite ((Cu, Ag, Zn)), and Osumilite (K–Na–Ca–Mg–Fe–Al–Si). Quantitative analysis showed that Osumilite (32.1%) and Barium Terbium Niobium Oxide (31.2%) were the predominant phases, followed by Freibergite (19.5%), Romarchite (11.4%), and Ziroite (5.8%).

The presence of sharp diffraction peaks indicate partial crystallinity, confirming the structural integrity of the nanoparticles and suggesting stability during storage and application Okwuego, *et al* (2025); Nwankwo *et al* (2025). Importantly, the identified mineral components may contribute physiologically relevant properties, such as blood clotting, tissue regeneration, and enzymatic activity, which could synergize with the bioactive phytochemicals from *Imperata cylindrica*. The XRD results demonstrate that the nanoencapsulation process preserves the crystalline mineral phases while integrating them into a stable polymeric delivery system, supporting both structural robustness and potential therapeutic functionality Ochie *et al* (2025).

ISSN 2278-2540 | DOI: 10.51583/IJLTEMAS | Volume XV, Issue II, February 2026

Table 6. Qualitative Analysis of Encapsulated Nanoparticles

Phase Name	Formula	Phase Details
Barium Terbium Niobium Oxide	Ba_2TbNbO_6	Minerals
Romarchite, syn	SnO	Minerals
Ziroite, syn	ZrO_2	Minerals
Freibergite, syn	(Cu, Ag, Zn)	Minerals
Osumilite	K–Na–Ca–Mg–Fe–Al–Si	Minerals

Table 7. Quantitative Analysis of Encapsulated Nanoparticles

Parameters	Weight Fraction (%)
Barium Terbium Niobium Oxide	31.2 (15)
Romarchite, syn	11.4 (7)
Ziroite, syn	5.80 (13)
Freibergite, syn	19.5 (4)
Osumilite	32.1 (7)

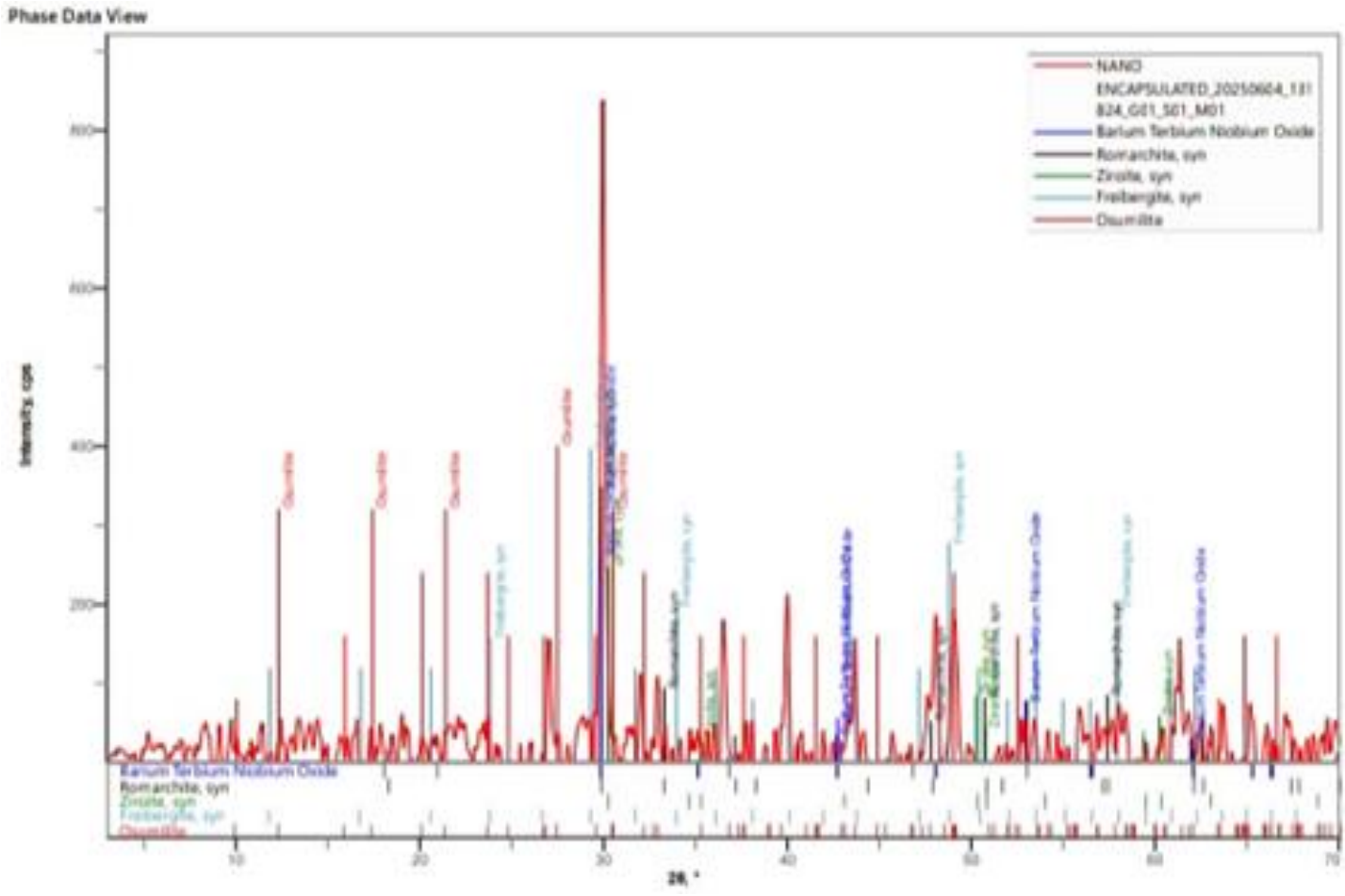

Figure 8 X –ray Diffraction spectral

ISSN 2278-2540 | DOI: 10.51583/IJLTEMAS | Volume XV, Issue II, February 2026

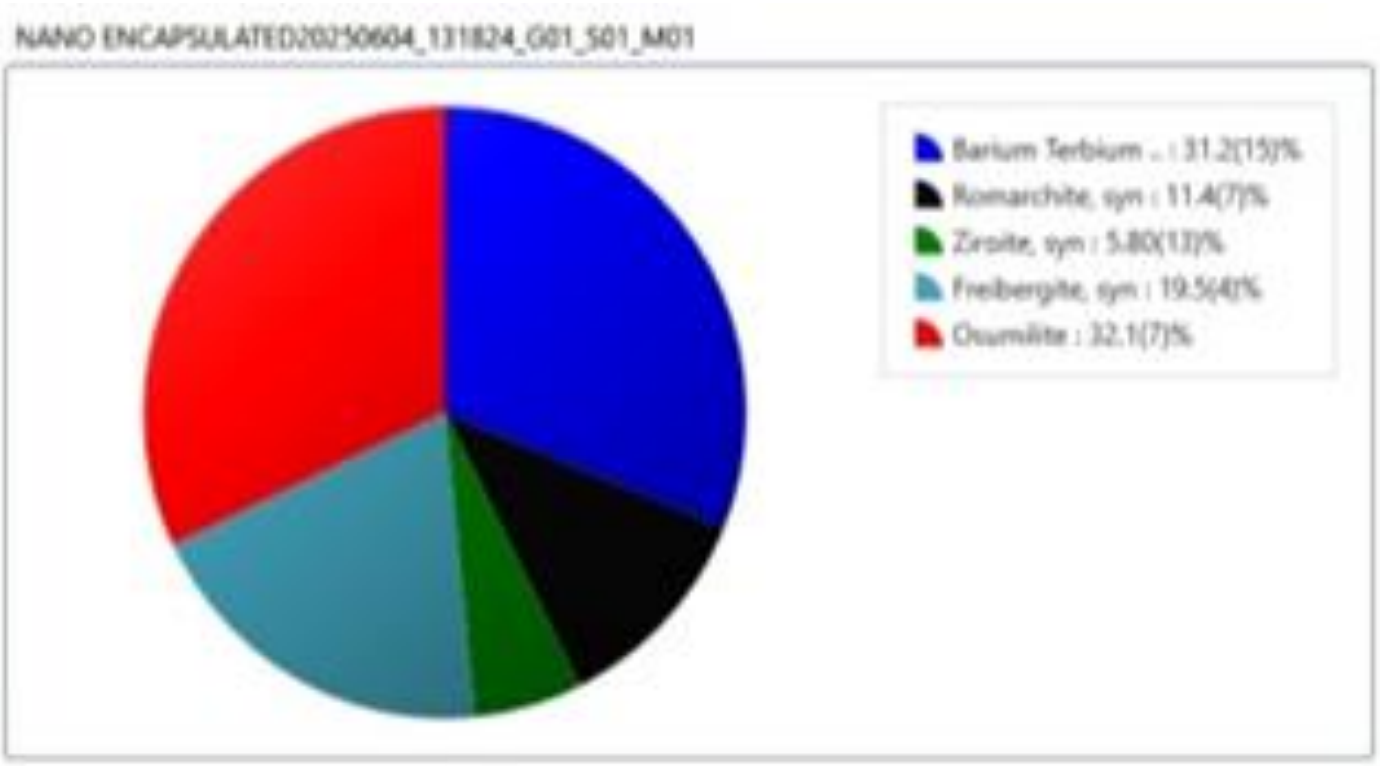

3.6 Phytochemical Profile and Therapeutic Relevance

Qualitative and quantitative phytochemical analyses confirmed that terpenoids (43.3%) were the dominant constituents of the methanolic root extract of *Imperata cylindrica*, followed by flavonoids (10.3%), tannins (5.7%), alkaloids (5.4%), and saponins (2.25%). These classes of secondary metabolites are well documented for their antioxidant, anti-inflammatory, antimicrobial, and hemostatic activities, which are critical therapeutic attributes for wound-healing applications Okwuego, *et al* (2025).

Table 8 Phytochemical screening results of Imperata cylindrica root extract

Phytochemical class	Test	Observation	Result
Alkaloids	Wagner's reagent	White precipitate	++
	Mayer's reagent	Reddish-brown precipitate	++
Saponins	Frothing test	Persistent frothing	++
	Emulsion test	Stable emulsion	++
	Fehling's solution test	Light reddish precipitate	+
Flavonoids	Ammonium test	Formation of green and light-green layers	++
	NaOH/Acetic acid test	Formation of green and light-green layers	++
Tannins	Ferric chloride test	Greenish-black precipitate	++
	Lead acetate test	Cream precipitate	++
Steroids and terpenoids	Ethanol–chloroform–H_2SO_4 test	Reddish-brown interface layer	++
Glycosides	Fehling's test	Opaque brick-red precipitate	++

+, slightly present; ++, moderately present; +++, present; −, absent.

Table 9 Quantitative phytochemical composition of Imperata cylindrica root extract

Phytochemical parameter	Amount (mg/4 g sample)	Percentage (%)
Tannins	0.057 ± SD	5.7
Flavonoids	0.103 ± SD	10.3

ISSN 2278-2540 | DOI: 10.51583/IJLTEMAS | Volume XV, Issue II, February 2026

Alkaloids	0.054 ± SD	5.4
Saponins	0.023 ± SD	2.25
Terpenoids	0.433 ± SD	43.3

Values are expressed as mean ± standard deviation (SD), where applicable.

Phytochemical analysis of *Imperata cylindrica* root extract (Tables 8 and 9) revealed alkaloids, flavonoids, tannins, saponins, steroids, terpenoids, and glycosides, with terpenoids being the most abundant (43.3%), followed by flavonoids (10.3%), tannins (5.7%), alkaloids (5.4%), and saponins (2.25%). These findings corroborate previous reports of high terpenoid and phenolic content, supporting the plant's antioxidant and pharmacological activities Okwuego, *et al* (2025); Mmuo *et al* (2024). The pronounced terpenoid content suggests potential for inflammation modulation and oxidative stress reduction, while flavonoids and tannins may contribute to antimicrobial activity and hemostasis. Alkaloids and saponins further enhance antimicrobial defense and membrane interactions. Nanoencapsulation within chitosan is expected to protect these bioactive constituents from degradation, allow controlled release, and preserve phytochemical integrity, demonstrating the extract's suitability as a stable, natural product-based drug delivery system with localized therapeutic efficacy.

CONCLUSION

The study successfully developed a chitosan-based nanoencapsulated formulation of *Imperata cylindrica* methanolic root extract, demonstrating structural integrity, preserved bioactive constituents, and nanoscale particle size. FTIR, UV-Vis, and XRD analyses confirmed retention of functional groups, improved phytochemical dispersion, and partial crystallinity of mineral phases, indicating stability and structural robustness. The encapsulated particles maintained acceptable organoleptic properties and exhibited potential for controlled release, enhanced tissue interaction, and therapeutic activity, including anti-inflammatory, antimicrobial, and antioxidant effects. These findings highlight the formulation as a promising natural product-derived nanoparticle system for topical wound-healing and hemostatic applications, with potential for further in vitro and in vivo validation.

REFERENCE

1. Agnihotri SA, Mallikarjuna NN, Aminabhavi TM (2004). Recent advances on chitosan-based micro- and nanoparticles in drug delivery. J Control Release. 2004;100:5–28. https://doi.org/10.1016/j.jconrel.2004.08.010.
2. Ahmed T, Aljaeid B (2016). Preparation, characterization, and potential application of chitosan metal nanoparticles in pharmaceutical drug delivery. Drug Des Devel Ther. 2016;10:483–507. https://doi.org/10.2147/DDDT.S99651.
3. Ali A, Ahmed S. A (2018) review on chitosan and its nanocomposites in drug delivery. Int J Biol Macromol. 2018;109:273–286. https://doi.org/10.1016/j.ijbiomac.2017.12.078.
4. Alonso MJ, Sánchez A. (2003) The potential of chitosan in ocular drug delivery. J Pharm Pharmacol. 2003;55:1451–1463. https://doi.org/10.1211/0022357022476.
5. Chen J, Guo Z, Tian H, Chen X.(2016) Production and clinical development of nanoparticles for gene delivery. Mol Ther Methods Clin Dev. 2016;3:16023. https://doi.org/10.1038/mtm.2016.23.
6. Chen LY, Chen Z, Wang CQ, Luo YH, Duan M, Liu RH. (2015) Protective effects of different extracts of Imperata rhizoma in rats with adriamycin nephrosis. J Chin Med Mater. 2015;38:2342–2346.
7. Cui J, Chao LL, You J, Xu XD (2012). Effects of Imperata cylindrica polysaccharides on glucose and lipid metabolism in diabetic mice. Food Sci. 2012;33:302–305.
8. Mmuo V.E and Okwuego P.O (2024) Spectrophotometric Determination Of Proximate, Vitamin B Complex and Elemental Contents of Pigeon Peas (Cajanus Cajan) Anachem Journal, 15(1), 85-95, DOI:https://doi.org/10.5281/zenodo.14567423
9. Nwankwo V, Okwuego P.O, Odika M (2025) Pesticide Levels in Two Fish Species from a Selection of the Niger River, Anambra state Nigeria**.** Asian Journal of Fisheries and Aquatic Research Volume 27 Issue 4 Pages 45-55

ISSN 2278-2540 | DOI: 10.51583/IJLTEMAS | Volume XV, Issue II, February 2026

10. Nkachukwu. M. B, Okwuego P. O, Ifeakor C. O, Offiah. V. O (2025) Spectroscopic Analysis of Leachables and Extractables from Selected Pharmaceutical Packaging: Assessing Ink and Adhesive Migration in Drug Labels and Containers in Nigeria. International Journal of Trend in Scientific Research and Development (IJTSRD) Volume 9 Issue 2, www.ijtsrd.com e-ISSN: 2456 – 6470 Nkachukwu. et al (2025)
11. Ochie O.S., Okonkwo S.I. P. O. Okwuego (2025) Synthesis and Characterization of Nanostructured Sorbents Derived from Rice Husks using FTIR, SEM, TEM and XRD Approaches. International Research Journal of Pure and Applied Chemistry Volume 26, Issue 1, Page 38-48; Article no. IRJPAC.129516ISSN: 2231-3443, NLM ID: 101647669
12. Okwuego P.O, Okonkwo S.I, Ekwonu A.M, (2021) Analysis of Structured natural sorbent from agricultural waste materials. International Journal of Chemistry and Chemical Processes E-ISSN 2545-5265 P-ISSN 2695-1916, Vol 7. No. 1 www.iiardpub.org Okwuego et al (2021)
13. Okwuego P. O, (2023) Optimization of oil spill cleanup using composites fibres (ES) modified kola nut pod. International Journal of Chemistry and Chemical Processes E-ISSN 2545-5265 P-ISSN 2695-1916, Vol 9. No.4 www.iiardpub.org
14. Okwuego P. O, Chigbo A Opara F.O,Oragwu I.P and Omoh T.O(2025) Spectral Characterization of Polyvinyl Acetate and It's Modified Mercury Complex, Exploring It's Structure and Applications. Research Journal of Pure Science and Technology E-ISSN 2579-0536 P-ISSN 2695-2696 Vol 8. No. 6. www.iiardjournals.org
15. Okwuego P. O, Okafor E.C, Okolo A.J, Anyanwu C.G (2025) Comparative Study of Engineered Bio-Sorbents Derived from Agricultural Waste. International Journal of Research and Innovation in Applied Science (IJRIIAS) ISSN NO. 2454-6194 doi.org/10.51584/IJRIAS Vol. 5. Issue 4
16. Okwuego, P.O, Offiah V.O, Nkachukwu, M.B, Ifeakor, C.O. (2025) Comprehensive Analysis of Leachables and Extractables from Pharmaceutical Packaging: Investigating Ink and Adhesive Migration in Selected Drug Products in Nigeria International Journal Of Research And Innovation In Applied Science (IJRIIAS) ISSN NO. 2454-6194 DOI **: https://doi.org/10.51584/IJRIASs.10040007**
17. Okwuego, P. O, Momoh, E. R**.** (2025) Phytochemical, Antioxidant and Antimicrobial Evaluation of Oil Palm Tree (Elaeis guineensis) Bark for Potential Nutraceutical and Pharmaceutical Applications International Journal of Health and Pharmaceutical Research E-ISSN 2545-5737 P-ISSN 2695-2165 Vol. 10. No. 11 2025 www.iiardjournals.org
18. Okorie E.A, Offiah V,O, Oragwu P.I, Okwuego P.O (2025) Assessment of Heavy Metals and Polycyclic Aromatic Hydrocarbons in Soil and Water in Selected Mining Areas of Ebonyi State, Nigeria. Journal of Global Ecology and Enviroment. Doi: 10.56557/jogee/v21i29123.